P2 AND P3 SPATIALLY SHAPED LASER SCRIBING OF CdTe AND a-Si THIN FILM SOLAR CELLS USING A 532 NM PICOSECOND MOFPA

Brian Baird[1], Tim Gerke[2], Kristopher Wieland[3] and Naba Paudel[3]

[1]Summit Photonics LLC, 5829 Jean Road, Lake Oswego, OR 97035 USA, [2]Fianium Ltd, 858 W Park Street, Eugene, OR 97401 USA [3]Department of Physics and Astronomy, University of Toledo, Toledo, OH 43606, USA

[1]Ph: +1 503 730 6631, email: brian.baird@summitphotonics.com, [2]Ph: +1 720 341 2784, email: tim.gerke@fianium.com, [3]Ph: +1 419 530 2654, email: kwielan@utnet.utoledo.edu, naba.paudel@rockets.utoledo.edu

ABSTRACT: Improved P2 and P3 scribing of thin film a-Si and CdTe solar cells are demonstrated using a 532 nm picosecond fiber laser with a square flat-top shaped beam profile at the work surface. The shaped beam profile optimizes the application of the available pulse energy and results in significantly faster scribe rates than achievable with Gaussian profiles. The uniform application of the fluence also improves scribe quality. The sidewalls are extremely straight and sharp and the absorber material is completely and uniformly removed from the underlying TCO with no damage to the TCO itself. Defects like cracking of the substrate or absorber edges, or peeling of the metal contacts are eliminated by the sharp profile edges of the flat-top beam and single pulse material removal.
Keywords: a-Si, CdTe, laser processing, thin film

1 INTRODUCTION

Continuous improvement and innovation in laser processing methods and laser architectures are needed to further improve device efficiencies and reduce overall device manufacturing costs. In particular, P2 and P3 laser scribes, which require the removal of CdTe and amorphous silicon (a-Si) absorbing layers, are widely performed by 532 nm Q-switched diode-pumped solid state lasers (DPSS) operating at nanosecond pulsewidth and employing conventional Gaussian beam delivery and focusing optics [1, 2]. Scribes produced with these laser systems often display undesirable sidewall non-uniformities, cracking, and excessive residual debris. Further, Q-switched DPSS laser architectures face scaling challenges as improvements in beam positioning technology demand laser performance at pulse repetition frequencies substantially higher than 200 KHz.

Increasingly, picosecond laser sources are being employed to meet the challenges of processing thin film and crystalline silicon (c-Si) photovoltaic (PV) devices [3]. The comparatively smaller heat affected zones produced by these sources in comparison to their nanosecond counterparts combined with higher peak power owing to their shorter pulsewidth have been shown to produce finer microfeatures with reduced melt effects. Beam shaping techniques are compatible with picosecond laser sources and have been widely employed in scribing of semiconductor devices [3] and more recently in scribing photovoltaic devices [4, 5].

In this work we evaluate CdTe and a-Si thin film photovoltaic device P2 and P3 scribe process performance and quality produced by 532 nm 30 picosecond pulses generated by a master oscillator fiber power amplifier (MOFPA) laser output operating at a pulse repetition frequency of 200 KHz. The pulses are spatially shaped through employment of diffractive optical beam shaping optics to produce a substantially uniform square imaged beam profile at the surface of the scribe layer at scribing speeds up to 7 m/s.

The laser source employed in this work was a commercially available Fianium Model HE1064/532 picosecond MOFPA producing 532 nm 30 picosecond pulses with a pulse repetition frequency of 200 KHz. A diffractive optical element was employed to transform the Gaussian spatial profile output by the MOFPA to a flat-top square spatial profile. This square spatial profile was subsequently imaged onto the surface of P2 and P3 CdTe and a-Si PV device samples to produce square beam imaged P2 and P3 scribes using a Summit Photonics laser workstation employing a hybrid galvanometer scanner-stacked linear stage beam positioning system.

2 EXPERIMENTAL SYSTEM

The laser processing system employed for spatially shaped 532 nm picosecond laser scribing of P2 and P3 CdTe and a-Si photovoltaic device samples is comprised of a Fianium Model HE1064/532 MOFPA laser system. The laser produces 30 picosecond pulses with energy per pulse up to 5 µJ at a 200 KHz pulse repetition frequency. A HoloOr refractive/diffractive optic was employed in this work to create a flat-top square beam at the work surface.

The HoloOr optic produces a 100 x 100 µm square beam profile at a distance of approximately 100 mm behind the shaper. A 90 µm square ceramic aperture was placed at the location of the 100 µm square beam profile to maximize profile edge steepness. The location of this aperture was imaged to infinity (collimated) using a lens at a distance approximately equal to that lens' focal length behind the aperture. A galvanometric scanner system equipped with 100 mm focal length telecentric scan lens then produces an image of the square aperture onto the work surface with a minification factor of 0.4. Figure 1 shows a block diagram of the experimental system employed.

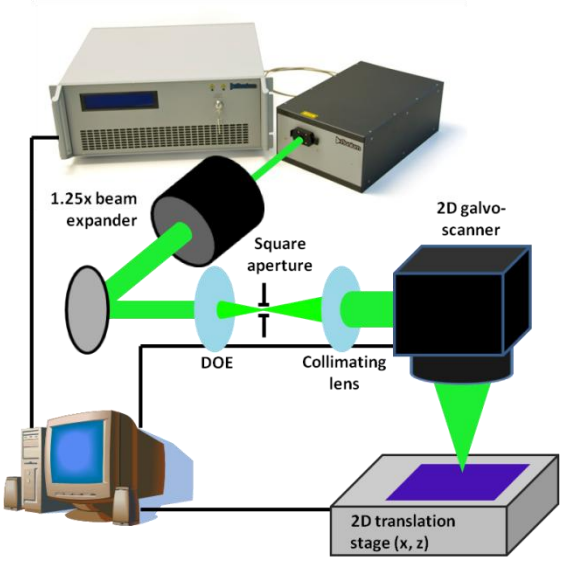

Figure 1: Schematic of the beam-shaping apparatus. DOE denotes the HoloOr flat-top beam shaper.

The shaped beam is input into a galvo-scanner head (Scanlab HurrySCAN II-14) that provides high speed, 2D control of image location on the work surface. The spatially shaped square image size at the work surface is approximately 40 µm on a side. Figures 2a and 2b demonstrate the substantial improvements in spatial beam uniformity and edge steepness for a square shaped beam in comparison to Gaussian spatial mode profile. The square shape shown in Figure 2a is rotated relative to true horizontal/vertical to precompensate for a slight rotation caused by the galvo-scanner.

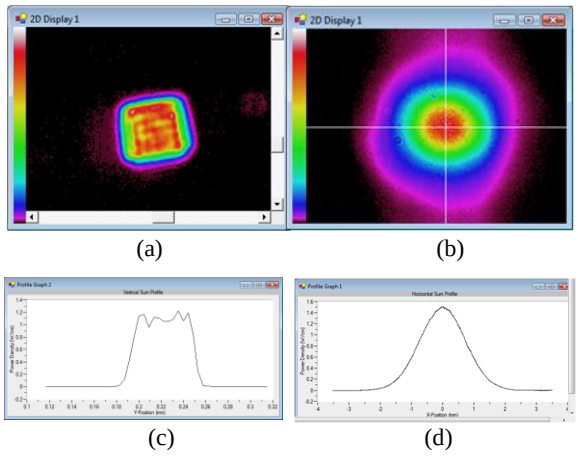

Figure 2: Typical 2D profiles of a) spatially shaped square beam and b) Gaussian beam employed in the present work. The profiles for the square and Gaussian beams are shown in (c) and (d) respectively.

3 CdTe SAMPLE PREPARATION

A detailed description of the device fabrication steps has been previously reported [6, 7]. To review, a TCO coated commercial glass (Pilkington Tec15® coated with highly resistive buffer layer) was cleaned and then layers of CdS (80-100nm) and CdTe (2.1 micron) were deposited via RF sputtering. The resulting films were wetted with MEOH saturated with $CdCl_2$. Films were then annealed in dry air for 30 minutes at 387°C. Back contacts were evaporated through a mask using a bi-layer of Cu (3 nm) and Au (20 nm). Finally, the devices were annealed at 150°C for 45 minutes. Devices created in this way have a typical efficiency of 12-13%. Figure 3 shows a simplified view of a CdTe photovoltaic device.

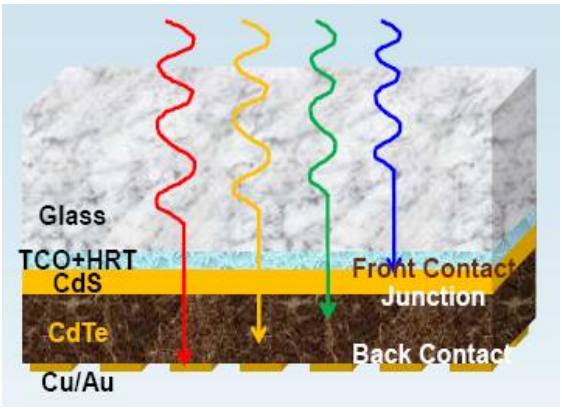

Figure 3: CdTe photovoltaic device construction.

4 P2 AND P3 a-Si and CdTe SCRIBING RESULTS

The CdTe samples prepared through the steps described above as well as the a-Si samples were next placed in the scribing system exhibited in Figure 1. The flat-top square beam profile (37x37µm) was imaged to the back surface of the samples (focusing through the glass substrate) to create P2 and P3 scribes using a back-side (superstrate) geometry. Figure 4 demonstrates the typical removal shape that is created using a single pulse from a shaped beam. The sidewalls are considerably straighter than would be for a Gaussian beam shape. The black spikes in this image and in other 3D confocal images are artifacts of having poor height information where the image intensity is very low. The confocal system used was an Olympus OLS 3100 laser confocal microscope.

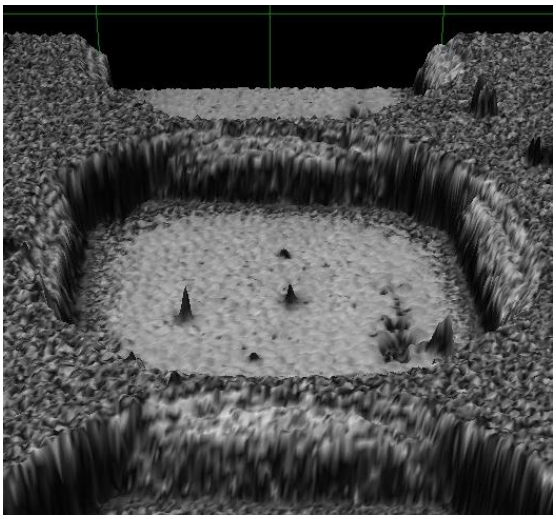

Figure 4: Square removal area created from a very high speed P3 scribe of a CdTe PV device utilizing a square flat-top shaped processing beam.

The material removal was conducted using a

backside process (superstrate) that involves an ablative lift-off. In a lift-off ablation, the laser energy is absorbed at the interface of the thick substrate and the layer(s) to be removed. The laser energy is absorbed and ablation occurs under the layer(s). The immense pressure from the ablated material causes the solid material above to be ejected from the device cleanly and with no heating-affects. Figure 5 demonstrates how the backside processing geometry works. The lift-off process allows large volumes of material to be removed with a single pulse but requires the substrate and all underlying layers to be transparent to the laser energy. The process is typically done with the laser beam impinging from above with the sample mounted upside down so that the removed material is pulled away from the sample by gravity and a standard debris removal system, and it results in extremely clean post-processed samples, even without washing.

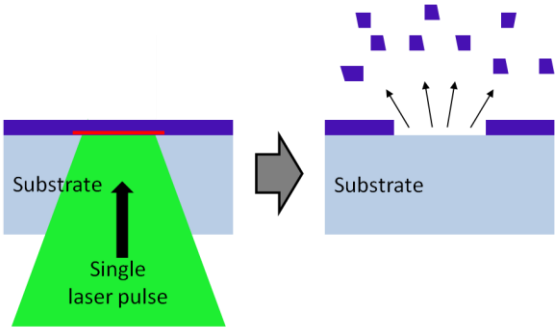

Figure 5: Diagram of a backside processing (superstrate, or lift-off) geometry. A single laser pulse ablates a small volume of material but results in removal of a much larger volume.

The first investigation was done to determine the threshold for ablation using the square beam. For this trial pulse energy was varied while all other parameters were held constant for a series of P2 and P3 scribes on both absorber materials. Figure 6 shows the result for a P2 CdTe substrate as a transmission microscope image, and demonstrates the ablation threshold condition of 0.11 J/cm^2 at the far right. As fluence increases from right to left the quality of the scribes quickly improves. All of the last four scribe results appear to be very good, which demonstrates a significantly wide process window. The fluence varies by approximately 50% for the four good scribes.

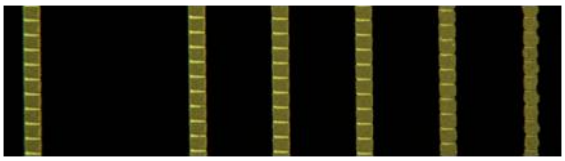

Figure 6: Transmission microphotograph of P2 scribes on CdTe with the square-beam shaping apparatus. Single pulses were used to scribe the individual squares, at a speed of 7000 mm/s, with laser pulse repetition rate of 200 kHz and fluences from 0.11-0.23 J/cm^2 (right to left).

At the ablation threshold, the pressure from ablation is barely sufficient for removal of the layers. At this energy the top layers quite often do not fully remove. They can either buckle but remain leaving a bulge, or they can remain partially attached and protruding upward, like a flake (most common in P3 scribe).

Figure 7 shows P3 scribes of a-Si devices and demonstrates a condition just above and just below the ablation threshold in Figure 7b (0.16 J/cm^2). Scribes at lower fluence values resulted in no visible material modification. The ablation threshold for the P3 substrates was slightly higher than that for P2 for both materials, and a slightly lower fluence value resulted in a buckling of the absorber and contact layer but was insufficient to fully remove the material.

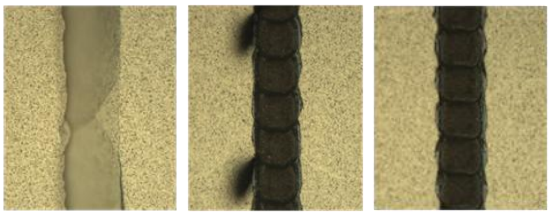

Figure 7: Reflection microphotographs of P3 scribes on a-Si with the square-beam shaping apparatus. Picosecond laser pulses at a repetition rate of 200 kHz were used to scribe the squares, at a speed of 7000 mm/s, and with fluences of a) 0.16, b) 0.18 and c) 0.23 J/cm^2.

A second important process parameter, and one that is expected to improve with the use of a square beam shape, is linear scribe speed. A square beam profile allows the scribe speed relative to spot size to be significantly increased because very little pulse-to-pulse overlap is necessary. The top half of Figure 8 depicts the results of P3 CdTe scribes with speeds ranging from 6000-9000 mm/s (right to left) made with a pulse fluence of 0.21 J/cm^2, and pulse repetition rate of 200 kHz from the picosecond fiber laser. The bottom half of the figure depicts the results of P2 a-Si scribes with speeds ranging from 1000-8000 mm/s (right to left) at a pulse fluence of 0.23 J/cm^2. P2 scribes of various speeds were also made and the optimal speed was determined to be 7000 mm/s for a fluence of 0.18 J/cm^2.

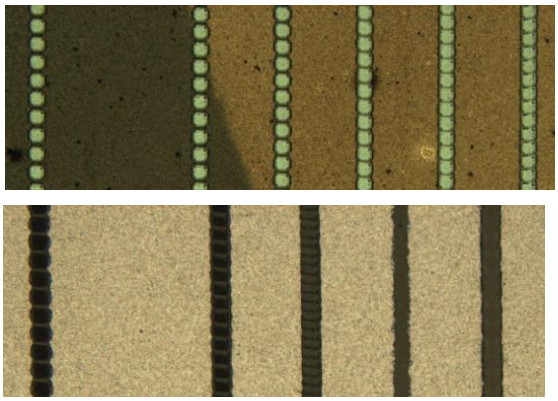

Figure 8: Reflection microphotograph of and P3 CdTe scribes (top) and P2 a-Si (bottom) with the square-beam shaping apparatus. Single pulses were used to scribe the CdTe (top), at speeds of 6000-9000 mm/s (right to left). The P2 a-Si was scribed at speeds of 1000-8000 mm/s (right to left), with laser pulse repetition rate of 200 kHz and fluence of 0.205 J/cm^2.

For comparison, we made another set of scribes using a significantly larger Gaussian beam (60 μm diameter)

and determined the optimal scribe speed to be around 5000 mm/s. The Gaussian beam also required nearly twice as much pulse energy than the square beam. This lower required pulse energy is unsurprising since the square beam applies virtually all of the available energy to the region to be removed. The Gaussian beam, on the other hand, applies a significant portion of the available energy to the overlap regions where it is wasted, and a significant portion of the energy is also located in the wings of the Gaussian where the fluence is insufficient for material removal.

Figure 9 compares the results of using a square beam and a Gaussian beam for scribes on a-Si and CdTe PV devices. Figure 9a and c are Gaussian beam scribes on CdTe and a-Si respectively and demonstrate the scalloped edges typical of such a beam shape. Figure 9b and d are similar scribes on CdTe and a-Si respectively, but using a square flat-top shaped beam instead. The improvement in the sidewall straightness is obvious. The top metal layer shows a small degree of irregularity, but the underlying absorber material is very straight, and both are significant improvements on the Gaussian results.

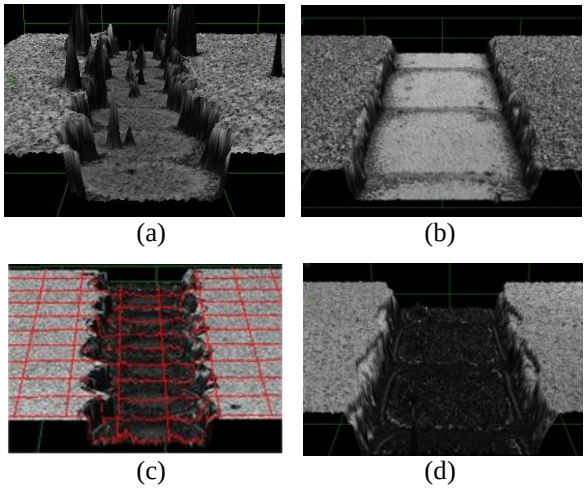

Figure 9: 3D confocal microscope images of a a) P2 scribe using a 20 μm Gaussian beam and b) P3 scribe using a 37 μm square-beam profile, both on CdTe PV devices. 3D images of a c) Gaussian beam P3 scribe and d) a square beam P2 scribe of a-Si.

The improvement in sidewall straightness can affect potential defects as well. The cusps of the scalloped sidewalls are an unwanted source of defects because their pointed aspect can lead to flaking and peeling of the top metal layer for P3 scribes. This excess material can result in shunts that significantly lower device efficiency or cause the devices to be completely defective. The extremely straight sidewalls and sharp edges of the square beam profile enhance the selective material removal and significantly lower the degree to which the peeling defects occur. Figure 10a demonstrates the peeling that can occur with conventional Gaussian beam scribing and Figure 10b shows the result with a square flat-top shaped beam. The square flat-top beam result demonstrates only a single small bump near the scribe edge, whereas the Gaussian result has many more pronounced features.

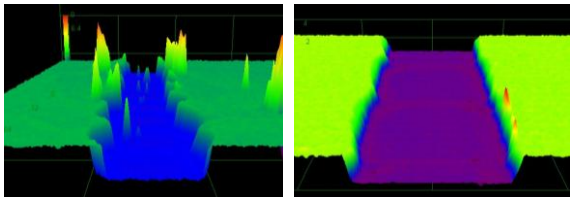

Figure 10: Confocal laser microscope 3D images of P3 scribes in CdTe using (a) a Gaussian beam and (b) a square flat-top shaped beam.

5 CONCLUSIONS

We have demonstrated the ability to scribe P2 and P3 CdTe and a-Si thin-film photovoltaic devices with 532 nm, 30 picosecond pulse fiber laser operating at 200 KHz employing a square flat-top spatial beam profile. The square beam creates scribes with significantly straighter sidewalls than achievable with a Gaussian beam. The sidewall straightness helps to limit scribe-related defects. The square flat-top beam profile was also shown to apply the available energy more optimally, which results in significantly faster scribe speeds than achievable with even twice the fluence in a Gaussian distribution. Linear scribe rates of 7000 mm/s were achieved with the square beam shape and less than 3 μJ of pulse energy. The scribe channels were completely free of absorber material with minimal or no damage to the underlying TCO. No visible detrimental heat-affects were observed.

6 REFERENCES

[1] J. Su, D. Tanner, and C. Eberspacher, Proceedings of 23rd European Photovoltaic Solar Energy Conference, pp. 2479-2481, Valencia, Spain (2008).
[2] J. Bonse, R. Patel, S. Manuef, R. Desailly, C. Devasia, and D. Clark, Proceedings of 23rd European Photovoltaic Solar Energy Conference, pp. 2325-2327, Valencia, Spain (2008).
[3] B. Baird, Proc. of SPIE, 7580, pp. 75800Q-1-75800Q-9 (2010).
[4] H. Huber, M. Englmaier, C. Hellwig, A. Heiss, T. Kuznicki, M. Kemnitzer, H. Vogt, R. Brenning, J. Palm, Proc. of SPIE, 7203, pp. 72030R-1- 72030R-9 (2009).
[5] E. Steiger, M. Scharnagl, M. Kemnitzer, 5th International Congress on Laser Advanced Materials Processing, Kobe Japan (2009).
[6] M. Shao, A. Fischer, D. Grecu, U. Jayamaha, E. Bykov, G. Contreras-Puente, R.G. Bohn, and A.D. Compaan, Appl. Phys. Lett., 69 pp. 3045-3047 (1996).
[7] S. Pookpanratana, X. Liu, N. Paudel, L. Weinhardt, M. Bär, Y. Zhang, A. Ranasinghe, F. Khan, M. Blum, W. Yang, A. Compaan and C. Heske, Appl. Phys. Lett., 97, pp. 172109-1 (2010).